OCCLUSION DETECTION IN DIGITAL IMAGES THROUGH BAYESIAN NETWORKS

Jorge Luís Nunes e Silva Brito - Ph. D.
The Military Institute of Engineering (IME), Brasil
Department of Cartographic Engineering - DE/6
jnunes@epq.ime.eb.br

Working Group IV/III.2

KEY WORDS: Occlusion Detection, Digital Photogrammetry, Bayesian Networks, Landscape and Image Maps, Geometric Modeling and Processing

ABSTRACT

Occlusions are a major obstacle for those dealing with the problem of automatically finding conjugate point pairs in overlapping images. They lead to mismatches or uncorrelated areas or features in the images. This is particularly critical in urban areas, where many mismatches generally occur, caused by relief-displacement of buildings.
This research addresses the problem of automatically detecting occlusions caused relief displacement in aerial, central perspective images.
In a more formal, mathematical approach, an occlusion corresponds to a linear geometric relationship of points in the image space to points in the object space, involving the image perspective center and two additional points, all three of which are collinear. The altered order relationship is easily checked in a deterministic approach. However, because there are errors involved in the computation of the image coordinates of the perspective center and in the projections of ground points back onto the image space, a simple Boolean test may misconstrue the significance of the apparent order relationship. These errors or uncertainties in the coordinates propagate along the photogrammetric process and suggest the use of a probabilistic approach for solving the problem of automatic detection of occlusions in digital images. A Bayesian Network is suggested, implemented and tested for that purpose.
The tests implemented show how a Bayesian network was successfully applied to the problem of automatically detecting occlusions in digital images. Three data sets, each of them containing 3D coordinates of point pairs, were used for testing: stereo-model measurements, simulated data, and digital orthoimage measurements.

1 INTRODUCTION

1.1 Occlusions in Digital Photogrammetry

Occlusions are areas of the earth not visible on remotely sensed images. The occurrence of those areas depends on the type of remote sensing system being used as well as on the type of energy being recorded.
As far as this research is limited to aerial, central perspective images, occlusions can be understood as areas of the ground not visible from one or both images (taken from different points of view) of the same geographic area. In those images, occlusions may occur for two reasons. First, they can be caused by shadows. These shadows can come from clouds, natural features such as trees, or from man-made features such as buildings. Second, occlusions may also occur because of the characteristics of the central perspective geometry itself. In the latter case, displacements of ground features occur along a radial line from the image nadir. These displacements may occlude other features along the same radial line.
Occlusions are a major obstacle for those dealing with the problem of automatically finding conjugate point pairs in overlapping images in the context of digital photogrammetry. They lead to mismatches or uncorrelated areas or features in the images.
The main principle for detecting occlusions in digital images is, at first glance, very simple: an orthoimage should be free of any parallaxes since it represents the orthogonal (or true) position of a point on the object space. Thus, given a pair of overlapping orthoimages, any residual parallaxes at a given point on the overlap area may be attributed mainly to errors in the DEM (which may be caused by occlusions in the original images), or to errors in the orientation parameters of these images. In fact, a number of investigations have used this principle. For example Doorn (1991) has associated a non-null matching vector to errors in the DEM. He also defined the geometric condition for the detection of occlusions. That condition will be used as a basis for occlusion detection using Bayesian networks later in this paper.

The strategy of using iterative orthophoto refinements to correct DEM's has been applied by Norvelle (1992). Li, Wang, and Li (1996) have presented a methodology for automatic quality diagnosis in DEM generation by digital image matching techniques. These researchers use the same principle of associating parallaxes in digital orthoimages either to errors in the DEM or to occlusions.
There is, however, a main drawback to the approaches mentioned. These approaches are deterministic, since they do not take into account errors associated with the planimetric positions of points in the digital orthoimages. Those errors are present in digital orthoimages by the error sources and their error propagation through the photogrammetric process. Therefore, the uncertainties in the planimetric coordinates of digital orthoimage pixels need to be taken into account in some way. This constraint suggests that a probabilistic approach would be more appropriate for detecting occlusions in digital images. Such an approach will be implemented using Bayesian networks, the principles of which are explained in the next sub-heading.

1.2 Bayesian Networks

Bayesian Networks have been used in many areas of knowledge since the late 1970s, particularly in artificial intelligence applications and knowledge representation and reasoning. In the context of spatial data, however, it remains a largely unexplored area, with few available references. An exception is a Doctoral dissertation entitled "*Bayesian Networks for Inference with Geographic Information Systems,*" which uses a Bayesian Network for modeling the problem of assessing the risk of desertification of some burned forests in the Mediterranean region (Stassopoulou, 1996). Judea Pearl (Pearl, 1988), one of the most active, contemporary researchers in this area, defines Bayesian Networks as directed acyclic graphs, in which the nodes represent random variables (regardless of the discrete or continuous domain), and the links represent causal influences among these variables. A detailed description of Bayesian Networks goes far beyond the scope of this paper. Those who are searching for literature in this topic will find also a comprehensive survey by Charniak (1991) in addition to the references mentioned above. For the purposes of this research, it is sufficient to summarize the principles of Bayesian Networks as follows:

- the nodes of the network represent random variables;
- a set of directed links connects pairs of related nodes;
- each non-root node (i.e., each node with parents) has a conditional probability matrix that quantifies the effects of the parents in the node;
- each root node (i.e., node with no parents) has a prior probability distribution, and
- the graph has no directed cycles (hence it is a directed, acyclic graph).

1.3 Statement of the Problem

Occlusion is a relationship of visibility, in the image space, along a given direction "θ", among the image perspective center and two points. It is caused by the relative position of those points mentioned above on the ground (object space). Figure 1 depicts an example of occlusion caused by relief displacement in a central perspective image.
Dorn (1991) stated how an occlusion can be detected along a single radial line in ideal images. He considered the relationship between the radial distances of two points in the object space and in the image space (i.e., points "A" and "B," and "a" and "b," respectively, in figure 1.
In the situation showed, point "B" is occluded by point "A" because its radial distance in the object space (R_B) is greater than (R_A), and the opposite situation is observed in the image space ($r_b < r_a$).
The problem stated above could easily be implemented in a deterministic approach. To do so, the following assumptions would be implicit:

- the images are ideal, which means they have no errors but relief displacement;
- the planimetric coordinates of ground points are assumed to be errorless, and
- the DEM from which the height of the ground points is interpolated is errorless.

Unfortunately the assumptions stated above are valid only theoretically. In real-world photogrammetric mapping projects, there are always errors in the computation of the coordinates of the perspective center "p" and in the projections of points "A" and "B" onto the image space. The uncertainties in the coordinates propagate according to the photogrammetric process. This characteristic suggests the use of a probabilistic approach to solve the

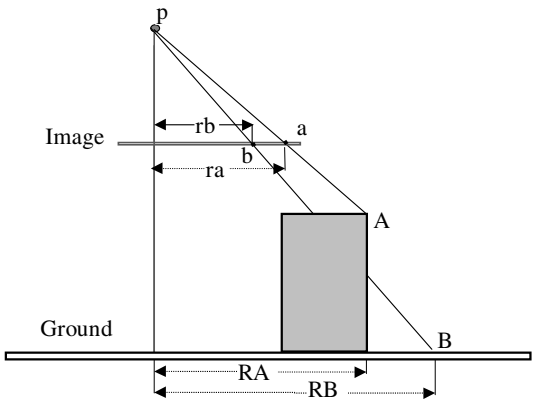

Figure 1. Occlusion along a single radial line in a vertical mage.

problem of automatic detection of occlusions in digital images. This can be implemented through a simple Bayesian network, which is described in the next section.

2 IMPLEMENTATION

2.1 Preliminary Steps

The first step to solve the problem of automatic detection of occlusions in digital images through a probabilistic approach is to take another look to figure 1, and changing it slightly. This modification is shown in figure 2.

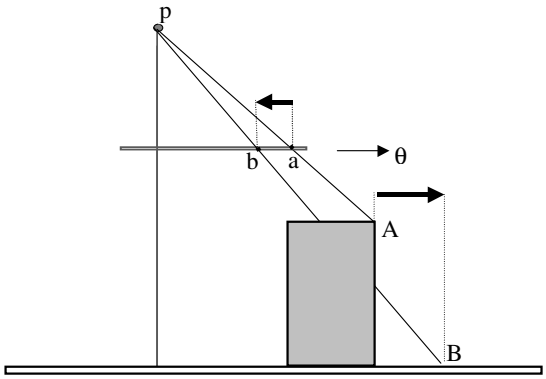

Figure 2. Lateral view of an occlusion along a generic direction of sight "θ" in a vertical image.

One can easily see from figure 2 that, if vectors **ab** and **AB** have opposite orientations, then "B" is occluded by "A." In that situation, the analysis of occlusion will consist in determining the probability of agreement in orientation between vectors **ab** and **AB**. Therefore, the problem of automatic detection of occlusions in digital images can be summarized in the answer to a "simple" question: **Do vectors "ab" and "AB" agree in orientation?** The answer to this question will be provided by the computation of the probability of agreement between **ab** and **AB** and, which comes from a simple Bayesian network. The differences between figure 2 above and its predecessor is that the vectors **ab** and **AB** determined from points "A" and "B", and their projections onto the image space are now being considered, instead of their respective radial distances, R_A , R_B, r_a, and r_b.

The approach described above is thought to be more efficient because it avoids some additional steps, necessary to compute the radial distances and the linearization of its formula, when propagating the error. Instead of computing vectors **ab** and **AB** only logical comparisons between the possible projections of "a" and "b" onto the " x' " axis will suffice for the occlusion analysis. This situation is illustrated in figure 3:

The geometric condition for checking for occlusions to be implemented in this research can then be re-stated as follows: given that X_B is greater than (or equal to) X_A in the object space coordinate system, if its projection (x'_b) onto the line of sight "θ" is less than that of "A" (x'_a), then "B" is invisible in the image space, because it is occluded by "A." This situation can be visualized through figure 2 above.

The implementation of the boolean statement described above requires the computation of the image coordinates of points "A" and "B" along the "θ" direction, x'_a and x'_b, respectively. This task requires an additional rotation, R(θ). This rotation is necessary to set the **x'** axis parallel to the line of sight, along which the existence of an occlusion will be investigated. This rotation determines a radial line parallel to the line of sight, as shown in figure 3. The following condition must be satisfied after that rotation:

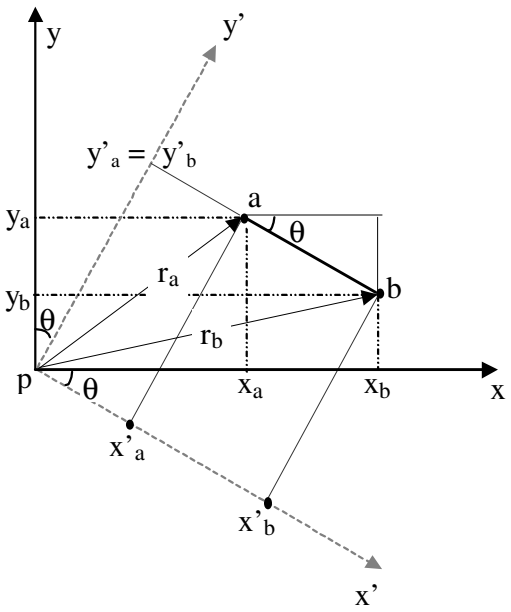

Figure 3. The image coordinate system (x, y) and its rotation according to the line of sight (**ab**) along which the occlusion will be investigated.

$$y'_a = y'_b \qquad (1)$$

The direction "θ" is computed from the image coordinates of "a" and "b," by equation 2:

$$\theta = \operatorname{atan}\left(\frac{|y_b - y_a|}{|x_b - x_a|}\right) \qquad (2)$$

The coordinates of points "a" and "b," along the **x'** axis, x'_a and x'_b, respectively, and their standard deviations constitute the input to the Bayesian network. These parameters are computed a mathematical model for assessing the precision of digital orthoimages (Brito, 1997). The preliminary steps described above can be summarized in the following algorithm:

// Algorithm for Data Preparation for Analysis of Occlusions through a Bayesian Network:

1) Select point pairs in the problem areas of original, digitized-frame images.
2) Compute ground coordinates of point pairs selected in step 1 above. // Either from stereo model or (orthoimage and DEM.)
3) Sort each point pair according to the "X" coordinate (ground coordinate system), so that $X_A \leq X_B$.
4) Project each point onto the digital image space through the collinearity equations, and compute the respective variance-covariance matrices (VCM's) projected points "**a**" and "**b**".
5) Compute the direction of sight (θ) for each point pair. The angle "θ" ranges from $-\pi/2$ to $+\pi/2$. It is computed by equation 2.
6) Rotate the coordinates of each point pair (equations 3 and 4) so that the condition $y'_a = y'_b$ (equation 1) is satisfied.
7) Compute the new VCM's for the transformed coordinates of the points in each pair, by the General Law of Error Propagation (equation 5).
8) Compute the eigenvalues of the transformed VCM's. // The computation of the eigenvalues is necessary to eliminate the covariance between x'_a and x'_b.
9) Output the values computed in steps 6 through 8 to a file, which will be read as the input for computation of the Bayesian network.

$$\begin{bmatrix} x' \\ y' \end{bmatrix} = R(\theta) . \begin{bmatrix} x \\ y \end{bmatrix} \tag{3}$$

$$R(\theta) = \begin{bmatrix} \cos(\theta) & \sin(\theta) \\ -\sin(\theta) & \cos(\theta) \end{bmatrix} \tag{4}$$

$$\Sigma\theta = \left(\frac{\partial R(\theta)}{\partial \theta}\right) . \Sigma yy . \left(\frac{\partial R(\theta)}{\partial \theta}\right)^T \tag{5}$$

Σyy is the respective variance-covariance matrix of the differential rectification process. (Brito, 1997).

2.2 Building the Bayesian Network

Before going through the set up of the Bayesian network itself, it is necessary to simplify figure 3. This simplification is achieved by drawing only the projections of "a" and "b" along the "θ" direction, x'_a and x'_b, respectively. Figure 4 shows these projections, associated with their respective error regions. These error regions are represented by elliptical areas of constant probability, centered at each point. The axis **x'** is enlarged for a better understanding of this situation.

It is important to notice that these elliptical areas above represent the joint distribution of the "A" and "B" coordinate errors, respectively, after the following transformations:

- projection onto the digital image coordinate system;
- rotation "θ" applied to "a" and "b" coordinates and to their respective VCM's, and
- computation of the eigenvalues of the rotated VCM's.

One can conclude from figure 4 that only the error distribution of the **x'** coordinate is necessary for implementation of the Bayesian network. This is because the occlusion is being investigated along that direction.

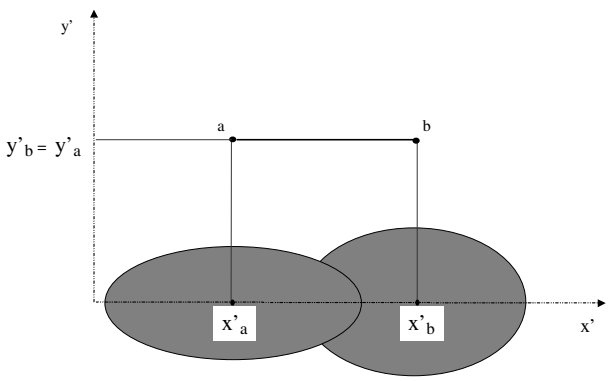

Figure 4. The Rotation of points "a" and "b" and their error distribution regions, represented by elliptical areas.

The general strategy in implementing the Bayesian network is to define a number of intervals, along the "θ" direction, for each one of the points forming the pair being analyzed. In this implementation, the ranges of the coordinates x'_a and x'_b were quantified into three intervals, which are sufficient to be used as a proof concept. However, there are no theoretical restrictions for this quantification. The Bayesian network corresponding to this situation can be schematically represented by figure 5:

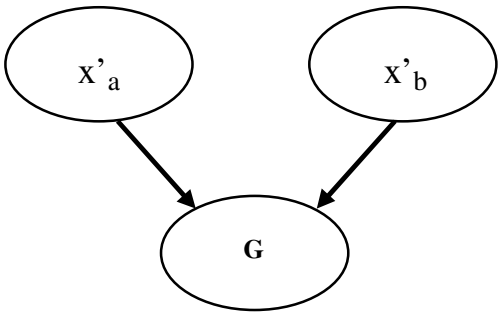

Variable States:

x'_a: (a_1, a_2, a_3)

x'_b: (b_1, b_2, b_3)

G: (Yes, No)

Where:

x'_a , x'_b: projection of "a" and "b" in "θ" direction;

G: Agreement between $\vec{ab}$ & $\vec{AB}$

Figure 5. Schematic representation of a Bayesian network for the implementation of the automatic occlusion detection problem.

The Bayesian Network will be set by evaluating both conditional and unconditional probabilities of agreement between **ab** and **AB** given every possible combination of x'_a and x'_b within the ranges. The final probability of agreement will be given by Bayes' Theorem, as follows in equation 6:

$$Pr(G) = \sum_i \sum_j Pr(G \mid a_i,b_j).\ Pr(a_i,).\ Pr(b_j),\ \ i, j = 1..3 \qquad (6)$$

$Pr(G \mid a_i,b_j)$ is the conditional probability of agreement between **ab** and **AB** (figures 3 and 4), given that x'_a belongs to the class interval "a_i", and x'_b belongs to "b_j", respectively, and $Pr(a_i,)$. $Pr(b_j)$ are the probabilities of x'_a and x'_b belonging to the class intervals "a_i" and "b_j", respectively. Figure 6 shows the relative positions of the points being considered as well as their respective class intervals, a_i, and b_j. Table 1 shows an example of the implementation of the problem of occlusion analysis between two points through a Bayesian network.

The computation of the conditional probability matrix for the Bayesian network must be performed dynamically because it depends on the relative position of the points being investigated. This characteristic distinguishes the problem being analyzed from most Bayesian network applications in a GIS context where the computation of the network is performed statically. As a logical consequence, the implementation must provide such a capability.

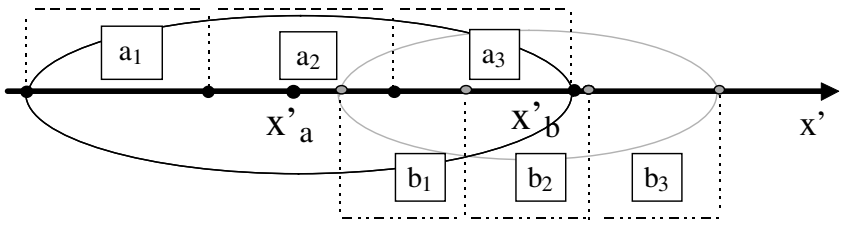

Figure 6. Projection of points "a" and "b" onto "θ" direction and their error distribution regions, represented by elliptical areas.

Interval "a_i"	Interval "b_j"	Pr ($G \mid a_i, b_j$)	Pr ($\neg G \mid a_i, b_j$)
a_1	b_1	1.0	0.0
a_1	b_2	1.0	0.0
a_1	b_3	1.0	0.0
a_2	b_1	MC^* (a_2,b_1)	1.0 - MC^* (a_2,b_1)
a_2	b_2	1.0	0.0
a_2	b_3	1.0	0.0
a_3	b_1	MC^* (a_3,b_1)	1.0 - MC^* (a_3,b_1)
a_3	b_2	MC^* (a_3,b_2)	1.0 - MC^* (a_3,b_2)
a_3	b_3	1.0	0.0

MC^* indicates that it is necessary to compute the conditional probability of agreement between a_i and b_j, e.g. through a Monte Carlo simulation.

Table1. Conditional probability matrix for occlusion analysis on the point pair shown in figure 6

2.3 Computing the Probabilities

2.3.1 Conditional Probabilities Pr($G \mid a_i, b_j$)

The computation of the conditional probability matrix of agreement between x'_a and x'_b, given that x'_a belongs to the class interval "a_i", and x'_b belongs to "b_j", respectively, depends on the relative position of x'_a and x'_b. These positions are random variables, since "A" and "B" can be located anywhere in the object space. This characteristic renders the dynamic aspect of the case being discussed. In practical terms, it means that the conditional probability matrix cannot be pre-computed and stored in memory for future use. Conversely, it needs to be evaluated for every pair of points being tested. More specifically, it is necessary to compute the probability of agreement of **ab** with **AB** given that x'_a is in range $\mathbf{a_i}$ and x'_b is in range $\mathbf{b_j}$, for i, j = 1,…,3. In other words, it is necessary to determine Pr ($G \mid a_1, b_1$), Pr ($G \mid a_1, b_2$), …, Pr ($G \mid a_3, b_3$). See figure 6 and table 1 above. As shown earlier in figure 3, **ab** has the same orientation af **AB** i.e., they agree whenever $x'_a < x'_b$,and, conversely, they disagree when $x'_a \geq x'_b$. The analysis of figure 6 supports the conclusion that one can be certain of agreement (i.e., Pr = 1) given ranges where $x'_a < x'_b$ throughout the whole domain. For example, Pr ($G \mid a_1, b_1$) = 1.0, since $x'_a < x'_b$ throughout a_1 and b_1, respectively. Similarly, Pr ($G \mid a_1, b_2$) = 1.0 , Pr($G \mid a_1, b_3$) = 1.0, and so forth. Therefore, it is necessary to investigate further the cases where there is an overlap between x'_a and x'_b ranges, i.e., to investigate Pr ($G \mid a_2, b_1$), Pr ($G \mid a_3, b_1$), and Pr ($G \mid a_3, b_2$). In these cases x'_a could be less or greater than x'_b. Therefore, it is necessary to estimate the probability of x'_a being less than x'_b. In other words, it is necessary to compute the conditional probability of agreement between **ab** and **AB** given that x'_a belongs to the class interval "a_i" and x'_b belongs to "b_j", respectively. This computation can be done either numerically or analytically. A numerical technique, namely the Monte Carlo simulation, was adopted for estimating the probabilities mentioned above. For instance, to estimate the first probability Pr ($G \mid a_2, b_1$), using the Monte Carlo simulation, random points for x'_a and x'_b are drawn uniformly within their corresponding ranges a_2 and b_1, respectively. The " x'_a " points that are less than x'_b are then counted and divided by the total number of points drawn, providing an estimate of the conditional probability.

2.3.2 Unconditional Probabilities Pr(a_i) and Pr(b_j)

Since there are uncertainties associated with the coordinates of the points being tested, it is necessary to compute the probability of x'_a and x'_b belonging to each of their respective class intervals "a_i" and "b_j". This requires choosing a probability distribution. It is also necessary to integrate this cumulative probability function within the limits of each interval. The central limit theorem provides mathematical support for choosing the Gaussian Distribution for the density probability function. This can be justified by the fact that the projections of ground points "A" and "B" onto the digital image space, "x_a", and "x_b", respectively, are random variables that can be expressed as a combination of "n" independent variables v_1, v_2, …v_n. The choice of interval amplitudes is another issue, directly related to the probabilities to be assigned to each interval. The following criteria were used to choose those intervals:
(1) the intervals should be symmetrically distributed around the expected values for x'_a and x'_b (see figure 8 below);
(2) a certain confidence level must be set. (This issue is discussed below) and;
(3) the integration of the Gaussian should be truncated so the probabilities (the areas under the Gaussian limited by each interval) add up to 1.0.

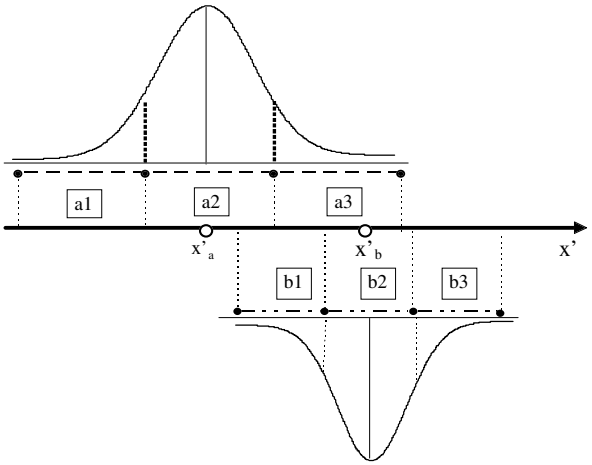

Figure 7. Criteria for choosing the probabilities
$Pr(a_i)$ and $Pr(b_i)$.

3 TESTS

The preliminary step for executing of the tests for occlusion detection was the selection and measurement of ground coordinates of point pairs in problem areas in the images. This task was performed in the digital photogrammetric workstation DPW 770. The same pair of aerial, digitized conjugate images at nominal scale of 1:12,500, over the region of Escondido, California, was used as the primary source of digital photogrammetric data.
The measurement of ground coordinates of testing point pairs in problem areas found in the images required that the ground coordinates of the testing points be manually measured in the stereo-model. They could not be automatically measured because of failures in automatic image matching procedures for finding conjugate point pairs in a digital image. This restriction stresses the importance of the investigation being developed.
A total of 26 point pairs were selected in the stereo-model, mainly along building corners. Besides the measurements in the stereo-model, it was also necessary to measure the same point pairs in the digital orthoimage in order to compare results. To do so, it was necessary to compute the height (Z) of the testing points from the DEM used to produce the orthoimage because only the planimetric ground coordinates (X,Y) can be obtained from the orthoimage.
A third data set was also generated. It has as its initial input the same ground coordinates as the stereo-model measurements. The difference between them is explained by including the imprecision of the DEM (σ_{DEM}) used for producing the digital orthoimage. Artificial errors were introduced in the projections of the stereo-coordinates onto the digital image space as a consequence of this action. This fact justifies why the name "simulated" was assigned to this data set. This data set was produced because of the deterministic nature of the results derived from the stereo-measurements. This problem will be explained later in the discussion of the results. After measuring the ground coordinates, it was necessary to compute the projections of the testing points onto the digital image space and their precision through their respective variance-covariance matrices. This task was executed by the mathematical model for error propagation through the photogrammetric processing.

4 DISCUSSION

The results of occlusion detection through a Bayesian network, for each of the data sets tested, were compared together. This comparison is represented by the Venn Diagram shown in figure 8:
The following conclusions can be drawn from figure 9:
(1) All the approaches agree in their respective analysis of occlusions for 15 out of 26 pairs, or 57.7% of the time;
(2) the stereo and the ortho image results agree in the same proportion as computed above;
(3) the simulated data and the orthoimage agree in 17 out of 26 pairs, or 65.4% of the time and;
(4) the simulated data and the stereo-model have produced the same analysis of results for 24 out of 26 pairs, or 92.3 % of the time.

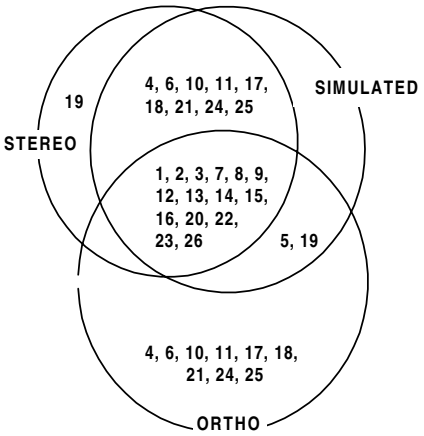

Figure 8. Venn Diagram showing the simultaneous analysis of occlusions for the 26 point pairs measured in the stereo-model, simulated data, and orthoimage.

It is worth mentioning that these statistics mentioned above were computed for both images simultaneously. If the comparisons were issued for individual images, the results would be even more encouraging. See, for example, the results depicted in table 2:

Image	STEREO *vs*. ORTHO	SIMULATED *vs*. ORTHO
I 10	(16 / 26) = 61.5%	(18 / 26) = 69.2 %
I 12	(22 / 26) = 84.6%	(22 / 26) = 84.6%

Table 2. Summary of the comparisons between single images

5 CONCLUSIONS

The results discussed above clearly indicate the feasibility of using a stochastic method (the Bayesian network) to deal with the problem of automatic detection of occlusions in digital images.
The following conclusions can also be drawn from the tests implemented with those data sets:
(1) identification of the causes of the occlusions can be solved by elimination. Such elimination depends on available knowledge about the images. For example, if a pair of points is known to be in an occluded area, but if it cannot be detected through the model, then the hypothesis of relief displacement (geometric disagreement) can be excluded. In that case, the occlusion can be attributed to shadows of buildings or clouds in the images;
(2) digital orthoimages can be used for occlusion detection analysis.
The most important conclusion, however, is the relationship between the analysis of occlusion performed by the implementation and the terrain itself. In other words, the terrain portrayed in the images "totally agrees" with the results of the occlusion analysis given by the implementation.

REFERENCES

Brito, J.L.N.S., 1997. Precision of Digital Orthoimages: Assessment and Application to the Occlusion Detection Problem. Doctoral Dissertation. The Ohio State University. Department of Geodetic Science and Surveying. Columbus, Ohio.

Charniak, E. 1991. Bayesian Networks Without Tears. In AI Magazine. Volume 12. Number 4. Pages 50 - 63.

Doorn, B. D., 1991. Multi-Scale Surface Reconstruction In the Object Space. Report Nr. 413. The Ohio State University. Department of Geodetic Science and Surveying. Columbus. Ohio.

Li, D., Shugen Wang, and Rongxing Li. 1996. Automatic Quality Diagnosis in DTM Generation by Digital Image Matching Techniques. In Geomatica, Volume 50. Number 1. Pages 65 - 73.

Norvelle, F. Raye. 1992. Using Iterative Orthophoto Refinements to Correct Digital Elevation Models (DEM's) . In The ASPRS/ACSM 92 Technical Papers. Volume 2. Pages 347 - 355.

Pearl, J., 1988. Probabilistic Reasoning in Intelligent Systems: Networks of Plausible Inference. Morgan Kauffmam Publishers Inc..

Stassopoulou, A. 1996. Bayesian Networks for Inference with Geographic Information Systems. Department of Electronic and Electrical Engineering. University of Surrey. Guilford, U.K.